Journal of Materials Chemistry B

ROYAL SOCIETY OF CHEMISTRY

PAPER

View Article Online
View Journal

Cite this: DOI: 10.1039/d5tb02613j

Elaboration of antibacterial polyurethanes for medical devices by a scalable process

Baptiste Caron,[ab] Marc Maresca,[c] Amélie Leroux,[b] Marie Lemesle,[b] Jean Louis Coussegal,[b] Loic Fontaine,[ab] Elizabeth A. Murphy,[def] Christopher M. Bates,[dg] Phong H. Nguyen,[h] Phillip A. Kohl,[de] Olivier Soppera,[ij] Stéphane Canaan,[k] Isabelle Poncin,[k] Yohann Guillaneuf[a] and Catherine Lefay *[a]

Medical devices are critical for patient survival in hospitals, yet they represent a leading cause of infections. Polyurethanes (PU), owing to their alternating hard- and soft-segment architecture, enable the fabrication of a broad spectrum of biocompatible materials from highly flexible to rigid and rank among the most prevalent polymers in device manufacturing. Conventional infection prevention relies on incorporating releasable antimicrobial agents into PU matrices; although straightforward to implement, these systems suffer from short-lived efficacy. Surface grafting of active molecules offers an alternative with superior longevity but entails protracted and expensive development. Here, we present a simple, effective, and industrially scalable process for producing antimicrobial PU grades tailored to biomedical applications. By dispersing and co-extruding just 2 wt% of an antibacterial copolymer within a PU matrix, we impart robust antibacterial properties without compromising mechanical performance. We further demonstrate compatibility with essential manufacturing additives, applicability across diverse PU grades, and crucially sustained bioactivity after three months of aqueous immersion or repeated bacterial challenges, all while maintaining non-toxicity. D-SIMS analysis provides the first direct molecular evidence of the antibacterial copolymer's incorporation in PU, revealing homogeneous bulk dispersion with preferential surface enrichment, ideal for contact-killing and unambiguous detection *via* the ^{127}I counterion despite minimal 2 wt% loading. This streamlined approach thus emerges as a compelling alternative to existing strategies, paving the way for safer and more reliable medical devices.

Received 24th November 2025,
Accepted 24th April 2026

DOI: 10.1039/d5tb02613j

rsc.li/materials-b

1. Introduction

Medical devices are essential in numerous hospital departments, including surgery, intensive care, obstetrics, and pediatrics. Common devices include catheters (venous, urinary, gastric), dressings, implants, and ventilators. However, their use is associated with a significant risk of healthcare-associated infections (HAIs), also known as nosocomial infections. These infections are primarily caused by pathogens such as *Escherichia coli*, *Staphylococcus aureus*, *Pseudomonas aeruginosa*, and *Staphylococcus epidermidis*, depending on the device involved.[1,2] Among the materials used in medical devices, polyurethanes (PUs) are particularly prominent.[3] These thermoplastic elastomers consist of alternating soft and hard segments, resulting in microphase separation that confers excellent and tunable mechanical properties. Combined with good biocompatibility, this makes PUs ideal for a wide range of applications, including catheters, implants, and ventilator components.[4] To mitigate device-related infections, manufacturers have developed antibacterial materials by incorporating active agents *via* coating or impregnation. Examples include antibiotics (*e.g.*, minocycline and rifampicin in Cook Medical's Spectrum®), antiseptics (*e.g.*, chlorhexidine in Teleflex's Chlorag + ard®), guanidine derivatives (*e.g.*, polyhexamethylene biguanide in B. Braun's

[a] Aix-Marseille Univ., CNRS, Institut de Chimie Radicalaire (UMR 7273), 13397 Marseille, France. E-mail: catherine.lefay@univ-amu.fr
[b] VYGON, Ecouen 95440, France
[c] Aix-Marseille Univ., CNRS, Centrale Marseille, iSm2, Marseille 13397, France
[d] Materials Research Laboratory, University of California, Santa Barbara, California, USA
[e] BioPACIFIC Materials Innovation Platform, University of California, Santa Barbara, California, USA
[f] Department of Chemistry and Biochemistry, University of California, Santa Barbara, California, USA
[g] Materials Department, University of California, Santa Barbara, California, USA
[h] Department of Chemical Engineering, University of California, Santa Barbara, California, USA
[i] Univ Haute Alsace, CNRS, IS2M, UMR 7361, F-68100 Mulhouse, France
[j] Univ Strasbourg, F-67000 Strasbourg, France
[k] Aix-Marseille Univ., CNRS, LISM UMR7255, IMM-UAR2044, 31 Chemin Joseph Aiguier, 13009 Marseille, France

Certofix®), or silver-based compounds (*e.g.*, silver sulfadiazine in Teleflex's ARROWg + ard® or silver ions in Edwards Lifesciences' Vantex CVC Oligon).[2,5] The efficacy of these systems relies on the sustained release of active agents. However, once depleted typically after a limited period the device loses its antibacterial activity and must be removed and replaced, a procedure often associated with secondary infections.[6] Thus, there is a critical need for durable, non-leaching antibacterial materials. Cationic biomaterials offer a promising solution.

By incorporating permanently bound cationic groups typically quaternary ammonium, sulfonium, or phosphonium onto the material surface, these systems kill bacteria upon contact by disrupting their negatively charged membranes. This contact-killing mechanism ensures long-term efficacy without reliance on agent release. Several cationic PUs have been developed and recently reviewed.[3] One approach involves synthesizing tailored PUs by incorporating either post-functionalizable[7–9] or inherently cationic monomers[10,11] into the polymer backbone. While effective, this strategy requires the development of entirely new materials, necessitating extensive regulatory validation before clinical use. An alternative is surface modification of existing PUs *via* ''grafting from'' or ''grafting to'' strategies. Techniques include plasma activation,[12] oxidation-induced grafting (using ozone, γ-rays, or electron beams),[13] isocyanate chemistry,[14] UV-induced polymerization,[15] or adhesive-assisted attachment (*e.g.*, *via* dopamine interlayers).[16] These methods have been comprehensively reviewed by Zhang *et al.*[17] Although effective in laboratory settings, they pose significant challenges for industrial scaling: multistep processes are time-consuming and costly, difficult to apply to complex geometries (*e.g.*, catheter lumens), and often require specialized equipment. Additional limitations include potential cytotoxicity (unreacted isocyanates), poor coating durability, and limited penetration into internal surfaces.[17]

To address these challenges, we have developed a scalable method based on the dispersion and co-extrusion of cationic diblock copolymers within commercial polymer matrices. After preliminary studies that allow to select the best antibacterial copolymer (microstructure block or statistical, cationic/hydrophobic monomer ratio, M_n, *etc. versus* Minimal Inhibitory Concentration (MIC) and innocuity), the quaternized poly(butyl methacrylate)-*block*-poly(dimethylaminoethyl methacrylate) PBMA-*b*-PDMAEMA (~20 kDa, 70 mol% DMAEMA), methyl-iodide-functionalized to bear permanent cationic charges was dispersed by extrusion into various polymer matrices.[18–20] This approach is simple, leverages well-established industrial dispersion processes, and is compatible with various thermoplastics. We previously demonstrated that only 2 wt% of this copolymer imparts robust antibacterial activity against *E. coli* and *S. aureus* in polyethylene (PE), poly(ethylene terephthalate-glycol) (PETG), and polylactide (PLA), without compromising mechanical properties.[20] The high molecular weight of the copolymer prevents its migration or leaching, ensuring long-term stability. A mechanical study using a propidium iodide assay confirmed the pore forming ability of the embedded copolymer at the surface.

Following our recent optimization of antibacterial testing protocols for PU (Pellethane® 2363-90AE),[19] the present work demonstrates the versatility and industrial relevance of this dispersion/co-extrusion strategy for antibacterial PU-based medical devices. We show that functional additives such as radiopaque $BaSO_4$ or colorants can be readily incorporated without loss of performance and that different type of PU (from soft to harder) can be turned into antibacterial equivalents. Moreover, the resulting materials exhibit sustained antibacterial efficacy during prolonged water immersion or repeated bacterial challenge, with no observed cytotoxicity. For the first time, depth-profiling dynamic secondary ion mass spectrometry (D-SIMS) confirms the presence of the antibacterial copolymer both at the surface and throughout the bulk of solid PU films (Fig. 1). This method thus enables the straightforward, large-scale production of durable, multifunctional, antibacterial PU medical devices suitable for long-term clinical use.

2. Experimental

2.1 Materials

Iodomethane (MeI, >99%, Acros), *n*-butyl methacrylate (BMA, 99%), 2-(dimethylamino)ethyl methacrylate (DMAEMA, 99%), and acrylonitrile (ACN, ≥99%, contains 35–45 ppm monomethyl ether and hydroquinone as inhibitors) were purchased by Sigma-Aldrich. BlocBuilder (>99%), an alkoxyamine based on the nitroxide SG1 (*N*-*tert*-butyl-*N*-[diethylphosphono (2,2-dimethylpropyl)]nitroxide) and the 1-carboxy-1-methylethyl alkyl moiety, and SG1 were provided by Arkema.

Methanol (MeOH, laboratory reagent ≥99.6%), diethyl ether (contains BHT as inhibitor, puriss. p.a., ACS reagent, reag. ISO, reag. Ph. Eur., ≥99.8%), 1,4-dioxane (anhydrous 99.8%) and 2-methyltetrahydrofuran (MeTHF, BioRenewable, anhydrous, ≥99%, inhibitor-free) were purchased by Sigma-Aldrich. Toluene (≥99.8%, HPLC Grade) was purchased by Fischer Chemicals. Tetrahydrofuran (THF, pure – stabilized with BHT) and *n*-pentane (Pure) provides from Carlo Erba. Pellethane® 2363 90 AE + 20% $BaSO_4$ was sent by the company Vygon® but the virgin polymer from Lubrizol and Blanc Fixe™ Xr-Hn Barium Sulfate was originally purchased from Venator®.

^{1}H spectra were obtained on a Bruker Avance DPX 400 MHz spectrometer. Tetramethylsilane (TMS) was used as internal standard. The ^{1}H chemical shifts were referenced to the solvent peak for $CDCl_3$ (δ = 7.26 ppm). SEC analyses were performed using an EcoSEC system from TOSOH equipped with a differential refractometer detector. THF was used as an eluent with 0.25 vol% toluene as a flow marker at a flow rate of 0.3 mL min^{-1} after filtration using Alltech PTFE membranes with a porosity of 0.2 μm. The column oven was kept at 40 °C, and the injection volume was 20 μL. One ResiPore Pre-column (50 mm, 4.6 mm) and two ResiPore columns (250 mm, 4.9 mm) from Polymer Laboratories were used in series. The system was calibrated using PMMA standards from Agilent in the range 602–520 000 g mol^{-1}. The SEC in DMF was performed using an EcoSEC instrument (Tosoh Bioscience) equipped with a solvent

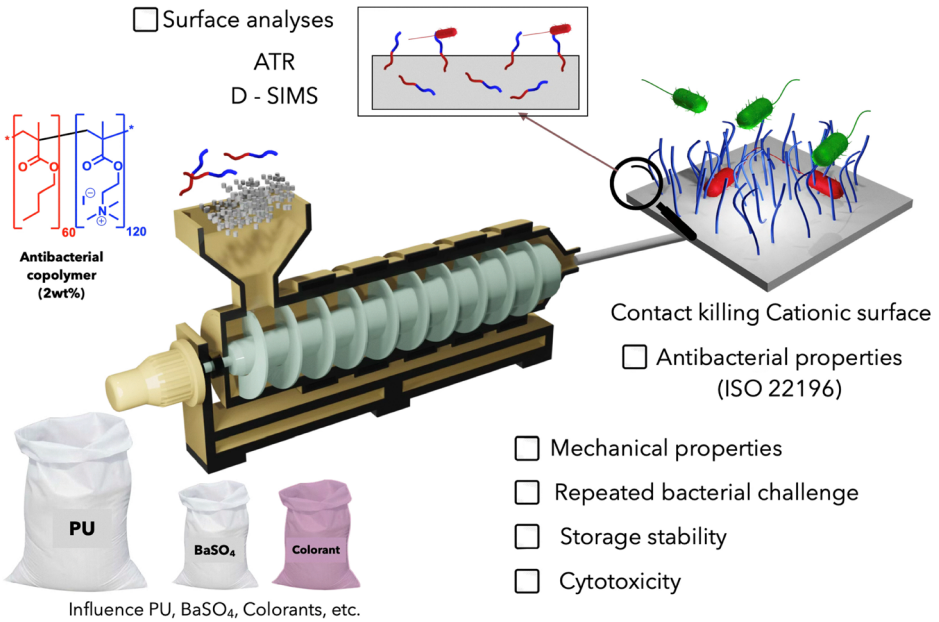

Fig. 1 Preparation of antibacterial polyurethane for biomedical applications *via* the dispersion and co-extrusion of antibacterial copolymer in PU matrix.

stocker, a dual flow refractive index detector and a UV detector. The stationary phase was composed of 2 PSS Gram columns (300 mm × 7.8 mm) (Agilent) and a PSS Gram precolumn (50 mm × 7.8 mm). The whole system was thermostated at 50 °C. The mobile phase was filtered DMF (0.2 µm Nylon membrane filter) containing 0.1 M of $NaNO_3$ at 0.7 mL min^{-1} for the sample part and 0.35 mL min^{-1} for the reference one. Samples were prepared at a concentration of 0.25 wt% in the mobile phase containing 0.25 vol% of toluene, as a flow marker. Samples were filtered through a 0.2 µm Nylon syringe filter before injection at a volume of 50 µL. Polymethyl methacrylate (PMMA) equivalent number-average and weight-average molar masses (M_n and M_w) and dispersities $Đ$ were calculated by means of conventional calibration curve established by using PMMA standards from 0.602 to 520 kg mol^{-1} (Agilent).

2.2 Copolymer synthesis and characterization

The synthesis and the characterization of the antibacterial copolymer (AB copolymer) follow the protocol described in previous work.[18,20] Briefly The antibacterial cationic PBMA-*b*-PDMAEMA diblock copolymer was prepared by a three-step procedure. The diblock copolymer was first prepared in a two-step procedure by nitroxide-mediated polymerization (NMP). At the end of the polymerization, the copolymer was recovered by precipitation in cold pentane. The composition in DMAEMA of the copolymer (F_{DMAEMA}) was determined by ^1H NMR in $CDCl_3$ (F_{DMAEMA} = 0.64) and the number-average molecular weight (M_n) measured by SEC/DMF (M_n = 18 400 g mol^{-1}). In a third step, the copolymer was quaternized with methyl iodide (MeI) to furnish the cationic antibacterial copolymer.

2.3 Elaboration of antibacterial PU films

The pre-blending step was performed with a HAAKE Rheomix OS internal mixer driven by HAAKE PolyLab OS Rheodrive 7 controller. PUR pellets were dried at 90 °C under vacuum for 4 h before extrusion. Once dry, 50 g of pellets were manually loaded into the internal mixer with 2 wt% of the antibacterial copolymer. The mixing was performed at 200 °C at 80 rpm for 3 min before recovering an antibacterial PU masterbatch that was cooled with liquid nitrogen before being crushed in a FRITSCH Pulverisette 19 universal knife mill to obtain mixture chips. The extrusion step was performed using a Thermo Scientific HAAKE MiniLab II mini-extruder. The pellets were dried at 90 °C under vacuum for 4 h before extrusion. Once dry, 5 g of masterbatch chips were manually loaded into the extruder. Extrusion was performed at 210 °C at 80 rpm.

For mechanical testing, tensile specimens (type 5A) were prepared by injection molding using a Thermo Scientific HAAKE Minijet II injector. Small pellets of extruded material were collected in the nozzle heated to 200 °C of the injector and then injected with a pressure of 500 bar in a test specimen mold (tensile bar ISO527-2-5A) heated at 60 °C. Bioassays were performed on circular shaped films of 3 cm diameter and 100 µm thickness. Upon exiting the extruder, the recovered rushes were cooled under air and then cut into small pellets and finally shaped using a Specac hydraulic press equipped with heating platens and a thin film kit. The pellets were pressed between two aluminum sheets heated at 170 °C and under 2 tons of pressure for 10 s.

2.4 Tensile tests

Tensile bars were analyzed using a Testometric TM M250-2.5CT bench coupled with the ''winTestTM Analysis''. Tests were carried out in accordance with ASTM D412, which describes a tensile test protocol adapted to rubber and elastomeric materials. This method consists of carrying out tensile tests with a drawing speed of 500 mm min^{-1} at ambient temperature and humidity. For each formulation, the Young's modulus and peak

stress values were extracted by taking the statistical mean of 5 tensile bars.

2.5 ISO 22196 antibacterial tests

The bactericidal activity of the PU materials was evaluated as previously described.[19] The bacteria used in the study were either Gram positive *Staphylococcus aureus*, ATCC CRM-6538P or Gram negative *Escherichia coli*, ATCC 8739. They were routinely grown on lysogeny broth (LB) agar plates. The bactericidal activity of the different matrices was evaluated according to an adapted ISO 22196 procedure. Briefly, reference and antibacterial films of 3 cm of diameter were sterilized (UV irradiation for 15 min). These samples were placed in a six-well plate before being overlaid with a 112 μL drop of a bacterial suspension containing 2×10^6 bacteria mL^{-1} in sterile water with 0.2 wt% NB or PBS. This drop was then flattened by a piece of Stomacher™ homogenization bag cut into a 2 cm square and UV sterilized beforehand, to increase contact between the bacteria and the surface being tested. Films were then incubated at 37 °C for 24 h before adding 5 mL of TSB to dilute the bacteria and stop the contact killing. This new mixture was added to a further 5 mL of TSB (1 : 10 dilution), followed by further dilutions to 1 : 100; 1 : 1000, and 1 : 10 000 in sterile water. 10 μL of each dilution were placed in a quarter of a Petri dish on an agar gel and then gently spread over the entire area. After one night at 37 °C, the number of colonies formed could be counted and the number of living bacteria determined. For each sample, the test was carried out in quintuplicate.

2.6 SEM analyses

Bacterial morphology on the different membranes was examined by scanning electron microscopy (SEM). Overnight cultures of *E. coli* ATCC 25922 and *S. aureus* ATCC CRM-6538P were adjusted to an optical density (OD) of 1 and then diluted to final concentrations of 2×10^3 CFU mL^{-1} for *E. coli* and 2×10^4 CFU mL^{-1} for *S. aureus*. An aliquot of 112 μL of each bacterial suspension was deposited onto the pristine PU and MAB-containing PU membranes and incubated for 1 h at room temperature. Bacterial growth was then arrested by fixation with 2% glutaraldehyde in 0.1 M cacodylate buffer (pH 7.2) for 1 h, followed by rinsing with the same buffer. No osmium tetroxide post-fixation was performed to avoid potential oxidative interactions between OsO_4 and the membrane-active material, despite the resulting lower contrast. Samples were subsequently dehydrated, dried, and sputter-coated with gold. SEM images were acquired using a FEI company Teneo (Thermo Fisher Scientific) scanning electron microscope operated at 2 kV in secondary electron (SE) mode under high vacuum, with magnifications ranging from ×1000 to ×10 000.

2.7 Elaboration of antibacterial PU films containing $BaSO_4$

Antibacterial PU films containing $BaSO_4$ were obtained in the same way as antibacterial PU films without $BaSO_4$, by replacing Pellethane 2363 90AE PU granules with Pellethane 2363 90AE B20 PU granules. These granules consist of a coextruded PU with 20 wt% $BaSO_4$ supplied by VYGON. Briefly, an initial mixture was made between Pellethane 2363 90AE B20 PU and 2 wt% of antibacterial copolymer in a HAAKE Rheomix OS internal mixer controlled by a HAAKE PolyLab OS Rheodrive 7 controller at 200 °C with a screw rotation of 80 revolutions per minute for 3 minutes. The resulting mixture was cooled in liquid nitrogen and reduced in a FRITSCH Pulverisette 19 universal knife mill. The masterbatch pieces were then extruded at 210 °C with a co-rotating intermeshing twin screw rotation of 80 rpm on a Thermo Scientific HAAKE MiniLab II mini extruder. The antibacterial and radiopaque PU rods were cut into granules and circular films 3 cm in diameter and 100 μm thick using a hydraulic press at 170 °C.

2.8 Elaboration of dyed antibacterial PU films

The dyed antibacterial PU films were obtained using the following process. Premixing in the internal mixer and grinding followed the same conditions as for conventional antibacterial PU materials. During extrusion, the masterbatch was coextruded with 2 wt% PE granules (violet masterbatch) at 210 °C with intermeshed co-rotating twin screws rotating at 80 rpm on a Thermo Scientific HAAKE MiniLab II mini extruder. The dyed antibacterial PU rods were cut into pellets and circular films 3 cm in diameter and 100 μm thick using a hydraulic press at 170 °C.

2.9 Antibacterial activity of water storage

Antibacterial PU films (disks with D = 3 cm, e = 100 μm) were stored in 3 mL of sterile water in 15 mL Eppendorf tubes for different periods of time before being tested in an antibacterial test in accordance with ISO 22196. Different storage times in water were studied (7, 24, 49, and 94 days) to determine the impact of a liquid medium on the antibacterial properties of the materials and the time before the active compounds can be extracted from the surfaces. The tests were performed in triplicate (n = 3). The storage waters were characterized to obtain the maximum inhibitory bacterial concentration (MIC) values. In 96-well plates, the wells were filled with 120 μL of MH and 30 μL of storage water, and 150 mL of bacterial suspension was added so that each column contained suspensions between 0 and 50 000 bacteria mL^{-1} by cascade dilution. The plates were incubated at 37 °C for 24 h and the MIC was detected by visual observation of bacterial colonies.

2.10 Repeated exposures tests against *E. coli* and *S. aureus*

The analyte surfaces (disks with D = 3 cm, e = 100 μm) were tested in an antibacterial test in accordance with ISO 22196. At the end of the test, the surfaces were washed by immersion in ethanol overnight and sterilized under UV light for 15 min. They were then subjected to a new test in accordance with ISO 22196. This process was repeated several times until the defined number of bacterial exposures (n = 4) as reached. This study was carried out in triplicate.

2.11 Hemolysis assays

The hemolytic activity of the solid antimicrobial materials was also determined. Briefly, 10 μL of human erythrocytes

suspension (8% in PBS) were then added per well of the sterile 96 well microplate containing the solid antimicrobial materials. After 60 min of incubation at room temperature, 90 μL of PBS were added and the microplate was centrifuged at 800 g for 5 min. 50 μL were then carefully collected and transferred to a new 96-well microplate and OD was measured at 405 nm. Hemolysis caused by copolymers was expressed as the percentage of hemolysis with Triton-X100 being used as a positive control.

2.12 Cytotoxicity assays

The toxicity of the materials was evaluated using human vascular endothelial cells (HUVEC cells obtained from ECACC, Sigma-Aldrich, Lyon, France), human skin keratinocytes (HaCaT cells obtained from Creative Bioarray, Shirley, NY 11967, USA), and mouse fibroblasts (L-929 cells (CCL-1™) obtained from ATCC, Molsheim Cedex France). Cells were routinely maintained on 75 cm^2 flasks in a CO_2 incubator at 37 °C in Dulbecco's modified essential medium (DMEM) supplemented with 10% fetal bovine serum (FBS), 1% L-glutamine, and 1% antibiotics (all from Thermo Fisher Scientific, Illkirch-Graffenstaden, France) for HaCaT and L-929 cells, or in endothelial cells specific medium (Sigma-Aldrich, Lyon, France) for HUVEC cells. To test the toxicity of the materials, cells were trypsinised, counted under a microscope using Malassez cell, and seeded at 30 000 cells per wells in 96-wells plates (100 μL per well). The next day, pieces of matrices (squares of 4 × 4 mm) were sterilely prepared from extruded films and were sterilely added into wells containing cells. Wells without matrices added and wells treated with Triton X-100 at 0.1% were used as untreated/negative and positive toxicity controls, respectively. After 48 h incubation, resazurin was added to each well at a final concentration of 30 μg mL^{-1} and cells were further incubated 1 h at 37 °C. The fluorescence intensity of the wells was then measured using a microplate reader (SynerMix, Biotek, Ex 530 nm/Em 590 nm). The fluorescence values were normalized by the untreated controls and expressed as the percentage of cell viability.

2.13 Dynamic secondary ion mass spectrometry (D-SIMS) analyses

Depth profiles were acquired using a Cameca IMS 7f Auto SIMS housed in the Microscopy and Microanalysis Facility of the Materials Research Laboratory at UC Santa Barbara. Prior to SIMS analysis, all samples were sputter-coated with a few nanometers-thick layer of gold prior to increase conductivity. An O_2^+ primary ion beam was rastered across a 65 × 65 μm^2 region to sputter samples at a rate of approximately 0.9 nm s^{-1}. $^{12}C^+$ was tracked as a control for carbon and $^{127}I^+$ was tracked as a proxy for copolymer concentration throughout the sample depths.

2.14 ATR analyses

IR spectra were acquired with a Nicolet IS50 FTIR spectrometer (Thermo Scientific) in ATR mode with a germanium crystal at a grazing angle of 64° (Harrick – VariGATR) corresponding to a analysis penetration depth of 0.66 μm. Data using a Diamond crystal (penetration depth of 2.01 μm) are given in SI (Fig. S3).

2.15 Small angle X-ray scattering (SAXS) analyses

Small-angle X-ray scattering (SAXS) measurements were performed using a custom-built, high-brilliance laboratory beamline at the BioPACIFIC Materials Innovation Platform, UC Santa Barbara. The instrument integrates a high-brightness liquid metal jet X-ray source (D2+, 70 kV; Excillum), an in-house–developed low-background scatterless slit beam collimation system, and a 4-megapixel hybrid photon-counting area detector (Eiger2 R 4M; Dectris) housed within a 3 m vacuum vessel. This configuration enables greater than tenfold reduction in data collection times compared to conventional lab-based SAXS/WAXS instruments, facilitating high-throughput nanostructural characterization across diverse sample types. Two-dimensional scattering data were azimuthally averaged to generate one-dimensional intensity profiles (arbitrary units) as a function of the scattering vector, $q = |\boldsymbol{q}| = 4\pi \sin(\theta/2)/\lambda$, where θ is the scattering angle and λ is the X-ray wavelength. Samples consisted of 100 μm-thick polymer films measured at room temperature without annealing to preserve their as-extruded nanostructure. Transmission-mode SAXS measurements were performed with a five-minute exposure time to characterize bulk morphology. Surface morphology was characterized using grazing-incidence SAXS (GI-SAXS) at an incident angle of 0.2°, near the critical angle for total external reflection, which limits the X-ray penetration depth to the top surface. GI-SAXS data were collected with a 30 minute exposure, enabling detailed analysis of near-surface nanostructures and anisotropic features.

3. Results and discussion

3.1 Antibacterial activity of the materials

As detailed in our previous report,[19] antibacterial polyurethane (denoted MAB in Fig. 1) was prepared by dispersing 2 wt% of quaternized PBMA-*b*-PDMAEMA copolymer within the PU matrix, followed by co-extrusion. After thorough melt-mixing to ensure homogeneous dispersion, a masterbatch was extruded and pressed into films (~3 cm diameter) using a hot press. This mixing step proved to be essential in the case of PUs to ensure the homogeneous dispersion of antibacterial copolymer in the matrix and reproducibility of the films. In fact, antibacterial tests against *E. coli* and *S. aureus* carried out on PU films containing 2 wt% of non-pre-mixed copolymer proved to be unreliable (statistically significant different values) and non-reproducible. This problem was solved by taking particular care during the copolymer dispersion stage. Unless otherwise specified (*e.g.*, when comparing different PU grades), this study focused on Pellethane® 2363-90AE. Antibacterial activity was assessed following ISO 22196 against *Escherichia coli* ATCC 8739 (Gram-negative) and *Staphylococcus aureus* ATCC 6538P (Gram-positive) as model pathogens.

A silver-zeolite-releasing PU (denoted AgION) served as a commercial benchmark. The ISO 22196 protocol was selected

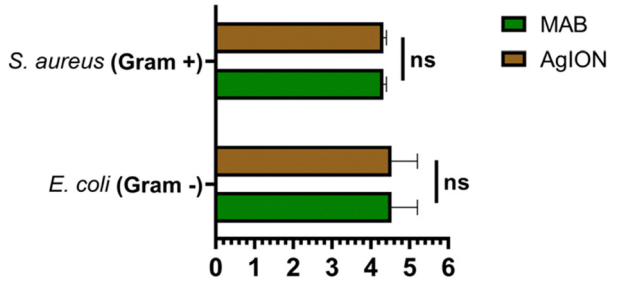

Fig. 2 Antibacterial efficacy of PU materials coextruded with 2 wt% of AB antibacterial copolymer (MAB, yellow) and AgION PU materials (brown) against the bacterial strains *S. aureus* ATCC 6538P and *E. coli* ATCC 8739 according to ISO 22196. Each average value is based on five different tests (n = 5). (ns: no significant).

due to its widespread use for evaluating antibacterial plastics. Testing was conducted on five independent films after 24 h bacterial contact. Efficacy was defined as a logarithmic reduction (Log Red) $\geq$ 3 relative to virgin PU, corresponding to $\geq$99.99% bacterial killing. For both strains, MAB exhibited high antibacterial performance (Log Red $\approx$ 4), comparable to AgION, with no statistically significant difference (Fig. 2).

The antibacterial mechanism of MAB-containing polyurethane (PU) materials is attributed to the disruption of bacterial cell membrane integrity. Upon contact with the material, MAB is proposed to alter membrane permeability and compromise membrane structure, leading to leakage of intracellular contents, denaturation of enzymes and proteins, and subsequent metabolic collapse, ultimately resulting in bacterial inactivation. Scanning electron microscopy (SEM) observations (Fig. 3) after 1 h of incubation revealed that *E. coli* and *S. aureus* retained their characteristic rod and spherical morphologies, respectively, when grown on pristine PU surfaces, indicating normal cell growth. In contrast, severe morphological damage, including cell rupture and collapse, was observed on the surface of PU containing 2 wt% MAB. These findings strongly support a membrane-disruption mechanism as the primary mode of antibacterial action.

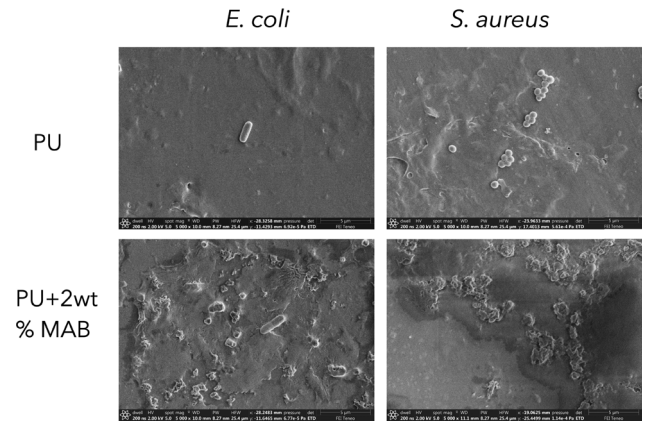

Fig. 3 SEM images of *E. coli* and *S. aureus* bacteria on the surface of PU and PU containing 2 wt% MAB after 1 h of contact.

3.2 Mechanical properties of the materials

Having confirmed the robust antibacterial efficacy of the materials, we next evaluated whether incorporation of the antibacterial copolymer compromises the mechanical integrity of the polyurethane (PU) matrix. Our objective is to generate an antibacterial PU variant that retains all native properties of the base material. Although we previously demonstrated that 2 wt% copolymer addition does not alter the mechanical behavior of LDPE, PETG, or PLA,[20] verification in PU was essential. Tensile specimens were injection-molded, and tests revealed no significant changes in Young's modulus or tensile strength upon copolymer incorporation (Fig. 4). Notably, the mechanical profile of the copolymer-modified PU (MAB) more closely resembled that of additive-free reference PU than the silver-zeolite counterpart (AgION). These results were confirmed by TGA analyses that revealed no significant difference between the degradation profiles (Fig. S1).

3.3 Compatibility with industrial medical-device processing

3.3.1. Incorporation of $BaSO_4$. Medical-device formulations frequently include functional additives beyond antimicrobial agents. Barium sulfate ($BaSO_4$), a radiopacifier, is routinely added at 20–25 wt% to enable X-ray visualization during catheter placement. This mineral filler needs to be incorporated in large quantities to have a significant effect and thus could be able to interact with the amphiphilic cationic copolymer. To assess potential interference with antibacterial performance, we co-extruded 2 wt% quaternized copolymer into Pellethane® 2363-90AE containing 20 wt% $BaSO_4$. Films were prepared as described and analyzed by SEM with and without the additive, confirming the homogeneous dispersion (Fig. S2). The films were then tested per ISO 22196. No

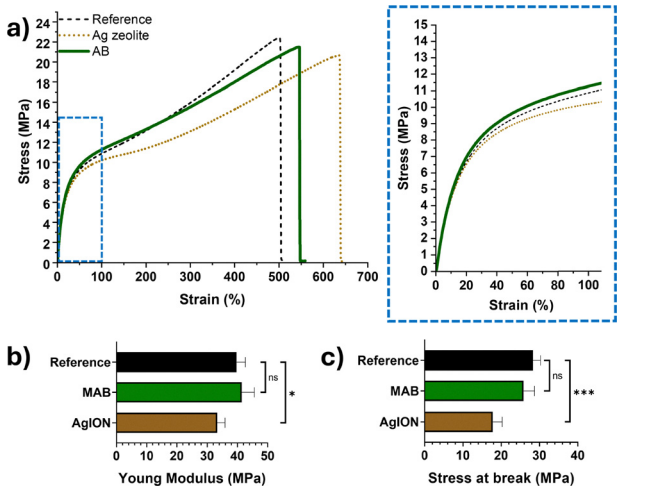

Fig. 4 Mechanical tensile stress analysis of test specimens made of PU (dashed black), PU AgION (dashed brown), and co-extruded PU with 2 wt% AB antibacterial copolymer (MAB, solid yellow) with (a) the associated tensile curves, (b) statistical comparisons of Young's moduli, and (c) associated tensile strength. Each element is derived from a series of four mechanical tests (n = 4). Statistical significance was obtained using ANOVA, comparing each sample with each other (*p < 0.05 and ***p < 0.005).

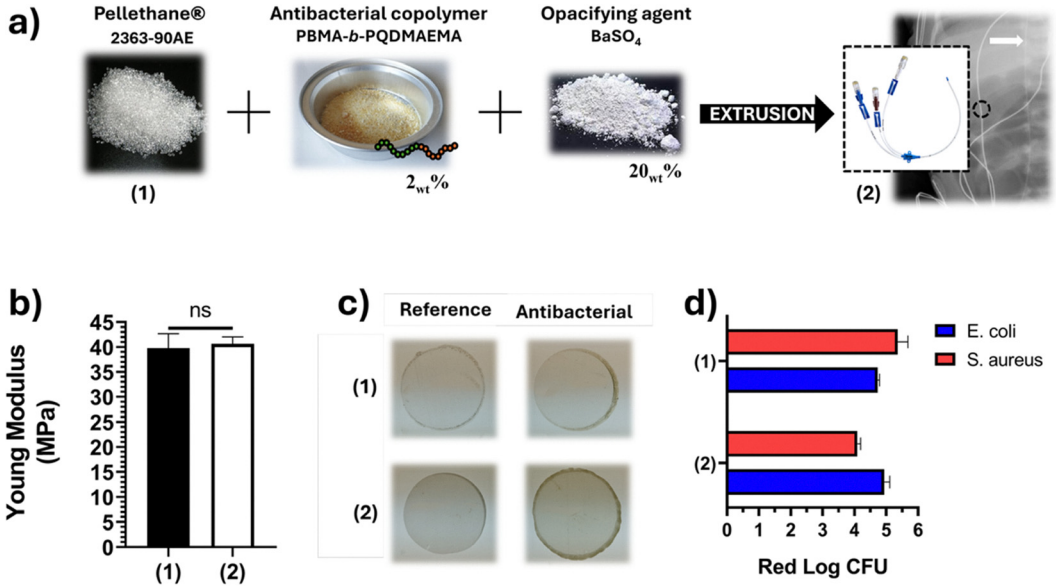

Fig. 5 Impact of 20 wt% $BaSO_4$ on MAB PU properties: (a) co-extrusion scheme; (b) tensile properties (n = 5; ANOVA); (c) surface appearance; (d) ISO 22196 antibacterial activity against *S. aureus* ATCC 6538P and *E. coli* ATCC 8739 with (2) or without (1) $BaSO_4$ (n = 3).

differences in Young's modulus, visual appearance, or antibacterial activity against *E. coli* and *S. aureus* were observed relative to $BaSO_4$-free controls (Fig. 5).

3.3.2. Incorporation of colorants. Colorants represent another widely employed class of additives in medical-grade polymers, primarily introduced to enhance visual differentiation among devices such as by size, diameter, or function and thereby establish intuitive color-coding systems that streamline clinical workflows, particularly in hospital settings where a diverse array of devices must be rapidly identified and deployed to meet patient needs. Industrially, these pigments are incorporated during material compounding in the form of color masterbatches, which consist of a carrier polymer loaded with a high concentration of dye; typically, approximately 2 wt% of such a masterbatch is blended into the base formulation to achieve the target hue without compromising processability or performance To evaluate the compatibility of our antibacterial copolymer with such colorants, we selected a representative purple MEVOPUR masterbatch (PE4M176082-ZT, polyethylene-based) as a model system.

Both 2 wt% of this colored masterbatch and 2 wt% of the antibacterial copolymer were simultaneously dispersed within a Pellethane 2363-90AE polyurethane matrix, followed by co-extrusion and compression molding into test specimens. As observed previously with radiopacifying fillers like $BaSO_4$, the inclusion of the dye had no discernible impact on antibacterial efficacy, with materials retaining full bactericidal performance as quantified in Fig. 6.

Given that such low loadings of colorants are well-known to exert negligible influence on bulk mechanical behavior, we did not repeat measurements of Young's modulus for these colored formulations; prior experience and literature consensus confirm that minor pigment additions at this level do not significantly alter stiffness, strength, or elasticity profiles. These results further confirm the robustness and additive-agnostic nature of the co-extrusion process, ensuring that essential aesthetic and functional modifications can be implemented without sacrificing the core antimicrobial protection of the final medical device.

3.3.3. Compatibility with different PU matrices. Polyurethanes (PU) were first discovered in 1937 by Bayer and are defined by the presence of urethane (carbamate, –NHCOO-)

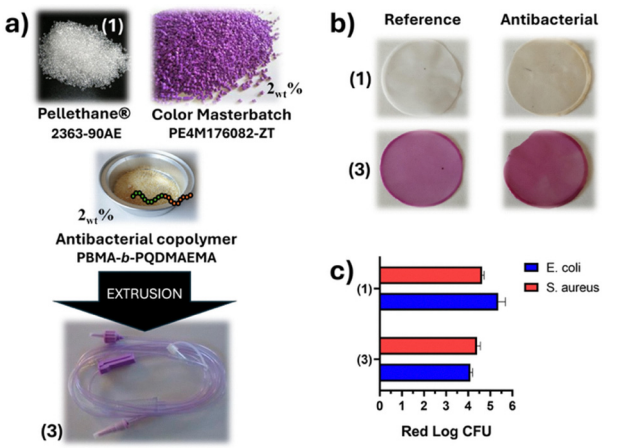

Fig. 6 Study of the impact of color masterbatch (2 wt%) on the properties of PU coextruded with 2 wt% of AB antibacterial copolymer (MAB): (a) formulation of a colorful antibacterial PU by coextrusion, (b) the visual effect of the presence of 2 wt% of AB antibacterial copolymer and color masterbatch on surfaces, and (c) study of the antibacterial power of antibacterial PU materials without (1) and with (3) 2 wt% PE4M176082-ZT purple color masterbatch against *S. aureus* ATCC CRM-6538P and *E. coli* ATCC 8739 according to ISO 22196 (the values shown are from a series of 3 tests (n = 3)).

and/or urea (–NHCONH–) linkages in their backbone. These materials have since become cornerstone polymers in the field of biomaterials due to their excellent biocompatibility, mechanical durability, and resistance to fatigue, as well as their remarkable compositional versatility, which enables the production of a broad spectrum of mechanical behaviors from highly elastomeric to rigid plastics depending on the specific formulation.[3] Chemically, PUs are synthesized *via* a step-growth polymerization reaction between diisocyanate and polyol monomers, typically in the presence of a chain extender (either a diol or diamine); the chain extender reacts with diisocyanates to form the rigid hard segments, while the polyol components generate the flexible soft segments, resulting in a multiblock copolymer architecture that gives rise to a complex, phase-separated morphology comprising alternating hard and soft domains.

To assess the versatility and broad applicability of our antibacterial modification strategy, we incorporated 2 wt% of the antibacterial copolymer into a series of industrial-grade PU matrices with distinct chemical compositions as detailed in Fig. 7.

Remarkably, the antibacterial performance remained consistently high across all tested matrices, with no statistically significant differences attributable to the underlying PU chemistry. In every case, the measured Log Reduction values exceeded 4, indicating strong bactericidal efficacy against both Gram-negative and Gram-positive strains. Furthermore, a slight but consistent trend toward higher activity was observed against *E. coli* compared to *S. aureus*, independent of the PU matrix, suggesting that the antibacterial mechanism is robust and largely insensitive to variations in polymer backbone structure or segment chemistry. These results underscore the generalizability of the co-extrusion approach, making it a highly adaptable platform for imparting durable, non-leaching antibacterial properties to a wide range of medical-grade polyurethanes.

3.4 Long-term material performance

3.4.1. Stability during aqueous storage. Many medical devices must retain efficacy for days to weeks in clinical use. A primary cause of activity loss in conventional antibacterial materials is the leaching of active agents. Silver-zeolite- or antibiotic-based systems rely on controlled release for bactericidal action, but this inevitably depletes the reservoir, reducing efficacy over time and limiting device lifespan. Moreover, released agents may induce toxicity or bioaccumulation in patients and the environment.

To assess the long-term stability of PU containing 2 wt% antibacterial copolymer (MAB), and thus that our high-molecular-weight copolymer remains entrapped within the PU matrix, we immersed film discs in sterile water for up to 3 months (Fig. 8a). Films were then retrieved at different intervals and evaluated for residual antibacterial activity per ISO 22196 (Fig. 8b).

ISO 22196 testing revealed that MAB PU maintained full antibacterial potency (Log Red $\approx$ 4) throughout the 3 month immersion period, unequivocally demonstrating the absence of copolymer leaching. In stark contrast, AgION PU exhibited progressive efficacy decline, dropping below the Log Red = 3 threshold after 2 months, a behavior consistent with silver-ion depletion reported in prior studies.[21]

Concurrently, storage water was challenged with serial bacterial dilutions; greater leachate concentration enables inhibition of higher inocula, yielding a maximum inhibited bacterial concentration (MICB) for each sample. The non-leaching activity was corroborated by these MICB assays on storage water (Fig. 8c).

Water from virgin PU and MAB samples displayed no inhibitory activity against *S. aureus* or *E. coli* at any time point, indicating negligible or undetectable release of bactericidal species. Conversely, AgION storage water inhibited bacterial growth within 7 days, with MICB values rising steadily over the

a)

	Polyurethane trademark	Hard segment	Macrodiol	Shore hardness	Supplier
1	Pellethane 2363-90AE	Aromatic	Polyether-urethane	90	Lubrizol
2	Pellethane 2363-80AE	Aromatic	Polyether-urethane	80	Lubrizol
3	Texin RxT80 A	Aromatic	Polyether-urethane	80	Covestro
4	Elastollan 1185 A	Aromatic	Polyether-urethane	85	BASF
5	Tecoflex EG 100A 93S	Aliphatic	Polyether-urethane	93	Lubrizol
6	Chronoflex C93S	Aromatic	Polycarbonate-urethane	93	Lubrizol

b)

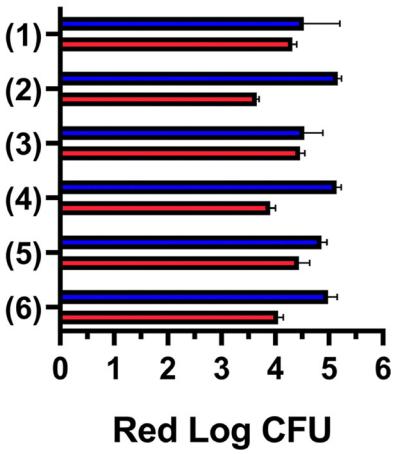

Fig. 7 Effect of the nature of the PU matrix used on the antibacterial activity of materials coextruded with 2 wt% of AB antibacterial copolymer: (a) characteristics of the different PU matrices used and (b) antibacterial activities against *E. coli* ATCC 8739 (blue) and *S. aureus* ATCC 6538P (red) depending on the PU matrix used. Each measurement corresponds to an average of 5 tests (n = 5).

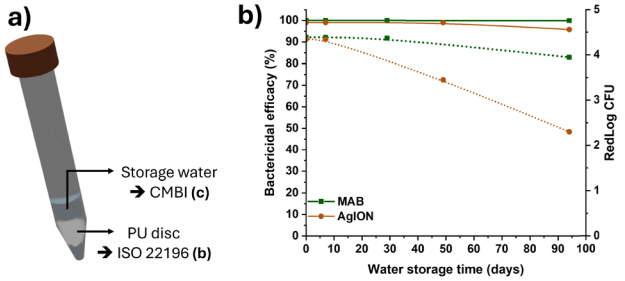

c)

Maximum concentration of inhibited bacteria MCIB (bacteria.mL^{-1})

Bacterial strain	S. aureus			E. coli		
Storage time (days)	1	7	21	1	7	21
Reference	0	0	0	0	0	0
AgION	0	12 500	12 500	0	1 560	50 000
MAB	0	0	0	0	0	0

Fig. 8 Study of the stability of antibacterial PU materials coextruded with 2 wt% of AB antibacterial copolymers (MAB) and AgION PUs, and the extractability of active species in an aqueous medium (schematized in a). (b) study of the preservation of the antibacterial properties (plain line bacterial efficiency and dotted line Red Log CFU) against *E. coli* ATCC 8739 of antibacterial discs after different storage times in water according to ISO 22196 (each measurement corresponds to the average of five tests (n = 5) and c) results of measurements of maximum concentration of inhibited bacteria (MCIB) with virgin PU used as reference.

initial 3 weeks, mirroring the observed loss of solid-phase activity in ISO 22196 tests.

Collectively, these data establish the superior temporal stability of copolymer-based MAB PU compared to release-dependent silver-zeolite systems. The non-leaching, contact-killing mechanism supports reliable performance for clinical applications requiring efficacy over periods of up to 3 months.

3.4.2. Resistance to repeated bacterial challenge. Although polyurethanes co-extruded with 2 wt% of the antibacterial copolymer have previously demonstrated no detectable release of the active polymer into the surrounding medium, concerns could still arise regarding the long-term stability of the antibacterial function. Specifically, the copolymer might undergo degradation over time, or its activity could be progressively masked for instance, by the accumulation of bacterial debris or biofilms on the surface potentially leading to a reduction in efficacy after repeated microbial challenges. To rigorously evaluate this possibility, we conducted a series of repeated antibacterial assays on the same set of MAB co-extruded PU discs, using both *E. coli* and *S. aureus* as model pathogens, in full compliance with the ISO 22196 standard protocol. Between each exposure cycle, the discs were carefully rinsed with ethanol and subjected to UV sterilization to remove residual bacteria and debris while preserving the integrity of the material. This challenge sequence was repeated four times under identical conditions (Fig. 9). Remarkably, regardless of the bacterial strain tested, no decline in antibacterial performance was observed across the four successive exposures.

These findings provide strong evidence that the antibacterial activity remains fully intact even after multiple microbial contacts and cleaning cycles, further validating the durability and reliability of PU materials incorporating this antibacterial copolymer.

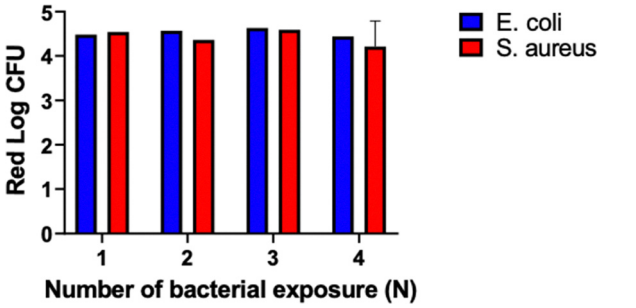

Fig. 9 Study of the stability of the antibacterial properties of PU materials coextruded with 2 wt% of antibacterial copolymer AB (MAB) as a function of the number of bacterial exposures to *E. coli* ATCC 8739 (blue) or *S. aureus* ATCC 6538P (red) to which it was exposed in accordance with ISO 22196. Each measurement corresponds to an average of 5 tests (n = 5).

3.5 Cytotoxicity assessment of the materials

To confirm that the surface-bound antibacterial activity of PU materials co-extruded with 2 wt% of the copolymer is truly selective for bacteria and does not adversely affect mammalian cells, we systematically evaluated the biocompatibility of these materials through a series of standardized cytotoxicity assays. First, we investigated hemolytic potential, a key indicator of blood compatibility for any material intended for medical device applications. Freshly isolated erythrocytes were suspended in contact with the material surfaces, and the extent of red blood cell lysis was quantitatively assessed by measuring the release of hemoglobin *via* colorimetric analysis at 540 nm (Fig. 10a). Subsequently, *in vitro* cytotoxicity was evaluated using three representative human and murine cell lines: HUVEC (human umbilical vein endothelial cells, Fig. 10b), HaCaT (human keratinocytes, Fig. 10c), and L929 (mouse fibroblasts, Fig. 10d). Cell viability was determined using a standard metabolic assay (*e.g.*, MTT or resazurin-based), with results expressed as a percentage relative to untreated controls. All experimental outcomes were benchmarked against virgin PU (unmodified polyurethane) as a negative control to establish baseline biocompatibility and Triton X-100 (TX100), a potent non-ionic detergent known for its membrane-disrupting properties, as a positive control to induce maximal cytotoxicity.

The results unequivocally demonstrate that PU materials incorporating 2 wt% of the antibacterial copolymer are neither hemolytic nor cytotoxic, with no statistically significant difference in biocompatibility between the modified and virgin PU across all assays ($p > 0.05$); specifically, hemolysis remained well below the 2% threshold considered safe for biomedical applications at a measured value of 0.6%, while cell viability consistently exceeded the 70% acceptance criterion for non-cytotoxic materials, reaching 93% (HUVEC), 98% (HaCaT), and 97% (L929).

In stark contrast, the positive control (TX100) induced near-complete hemolysis (~100%) and reduced cell viability to approximately 2% across all cell types. These findings robustly confirm the bacteria selective nature of the antibacterial mechanism and prove the excellent biocompatibility of the

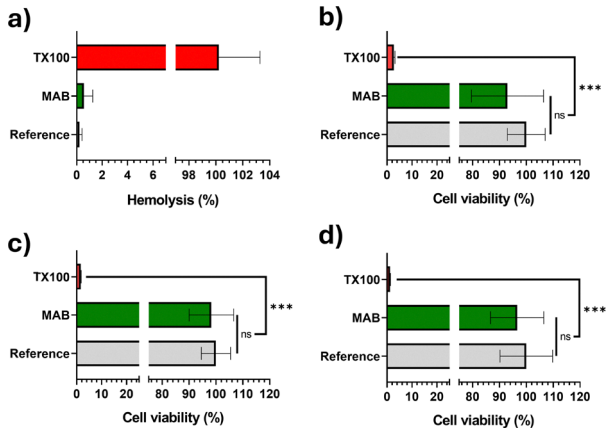

Fig. 10 Safety studies of PU materials coextruded with 2 wt% of AB antibacterial copolymer: (a) measurement of the hemolytic power of the material and cytotoxicity studies on cell lines (b) HUVEC, (c) HaCaT, and (d) L929 fibroblasts. Negative controls on PU materials without AB antibacterial copolymer and positive controls on TX100 were also performed. Each measurement corresponds to the average of three tests (n = 3). Statistical significance was obtained using ANOVA, comparing each sample with each other (***$p < 0.005$).

co-extruded PU materials, satisfying critical regulatory benchmarks for safe use in medical devices.

3.6 Characterization of the material surface

Although ISO 22196 testing unequivocally demonstrates the robust antibacterial efficacy of PU materials containing 2 wt% of the antibacterial copolymer, direct detection and spatial localization of this additive within the bulk or at the surface remain technically challenging. Such characterization is not only scientifically valuable for elucidating the precise mechanism of action and optimizing bacterial killing efficiency but also critically important from a regulatory and quality control perspective, where proof of additive presence, distribution, and stability is often required for medical device approval.

In our prior investigation[20] involving the same antibacterial copolymer dispersed at 2 wt% into polyethylene (PE), polylactic acid (PLA), and polyethylene terephthalate glycol (PETG) matrices, we employed a suite of advanced surface-sensitive techniques to probe its localization. Specifically, time-of-flight secondary ion mass spectrometry (ToF-SIMS) was applied to surfaces of PETG, LDPE, and PLA samples; additionally, atomic force microscopy (AFM) in tapping mode and nano-infrared spectroscopy (nano-IR) which enables spatially resolved Fourier transform infrared (FTIR) mapping with nanoscale lateral resolution were used to characterize LDPE film surfaces. Despite the high sensitivity and chemical specificity of these methods, none yielded unambiguous evidence of the copolymer's presence or phase segregation at the material surface, likely due to its low overall loading, fine dispersion, and chemical similarity to the host polymers.

This challenge is even greater in the polyurethane system, where the task of distinguishing the additive from the matrix is even more formidable. Both the antibacterial copolymer and the PU backbone share a predominantly carbon-based skeleton with oxygen and nitrogen heteroatoms, resulting in nearly overlapping spectroscopic signatures. Moreover, with only 2 wt% of the copolymer uniformly dispersed throughout the entire volume of the material rather than being enriched or immobilized exclusively at the surface the expected surface concentration is theoretically minimal, further reducing the signal-to-noise ratio in surface-probing techniques.

Consistent with these expectations, attenuated total reflectance (ATR) FTIR analysis revealed no detectable spectral differences between virgin PU and its counterpart loaded with 2 wt% antibacterial copolymer (Fig. 11 and Fig. S3).

Even if there is very slight differences at 1180, 1100 et 1070 cm^{-1}, the absence of distinct vibrational bands attributable only to the additive underscores the intimate blending and chemical compatibility achieved *via* co-extrusion, while highlighting the limitations of conventional spectroscopic tools for verifying low-level, chemically similar inclusions reinforcing the reliance on functional (*i.e.*, antibacterial) performance as the primary metric of success in this system.

To gain deeper insight into the morphology and spatial distribution of the antibacterial copolymer within the PU matrix, we performed small-angle X-ray scattering (SAXS) experiments (Fig. 12). These analyses attest that the diblock copolymer was successfully integrated into the overall network structure without disrupting the microstructure of the polyurethane. Furthermore, grazing-incidence SAXS measurements were in excellent agreement with transmission SAXS, demonstrating that the antibacterial copolymer is distributed through the film thickness (data in SI). To further evaluate how processing conditions influence copolymer distribution and film nanostructure in PU, we compared two strategies: the standard protocol involving pre-compounding into a masterbatch prior to co-extrusion *versus* direct addition of 2 wt% copolymer during extrusion (without pre-mixing) (Fig. 12 and Fig. S4–S6

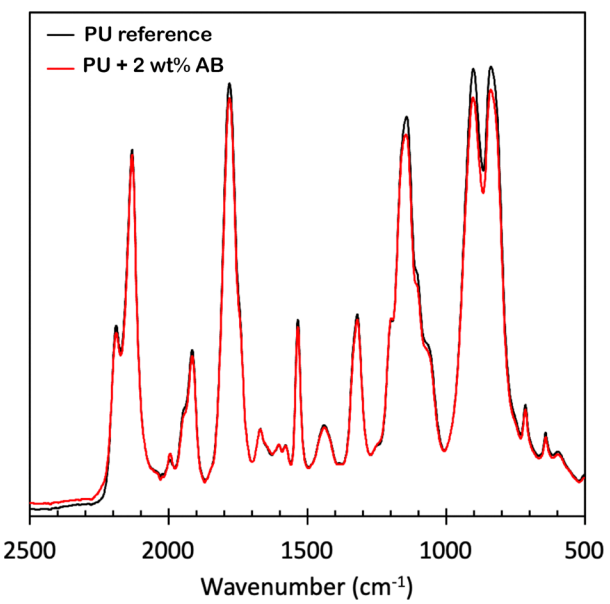

Fig. 11 ATR analyses (Ge crystal) of PU without (black) and with 2 wt% of antibacterial copolymer (red).

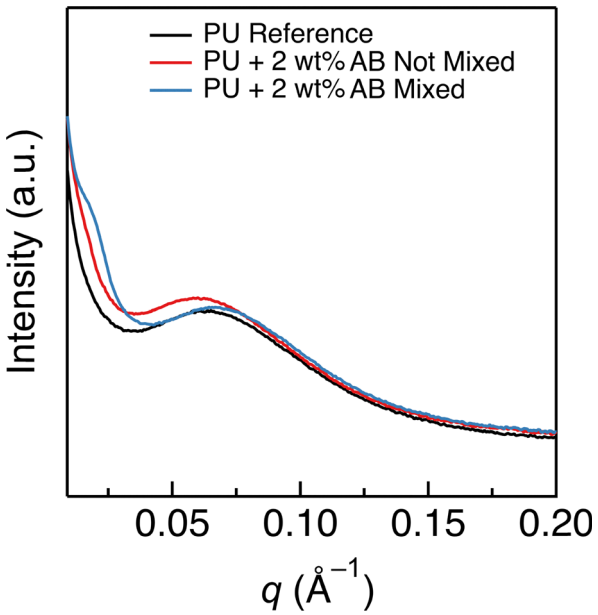

Fig. 12 SAXS analyses (transmission mode) of PU without (black) antibacterial copolymer and with 2 wt% of copolymer with no premixing (red) and with premixing (blue) as used in this work.

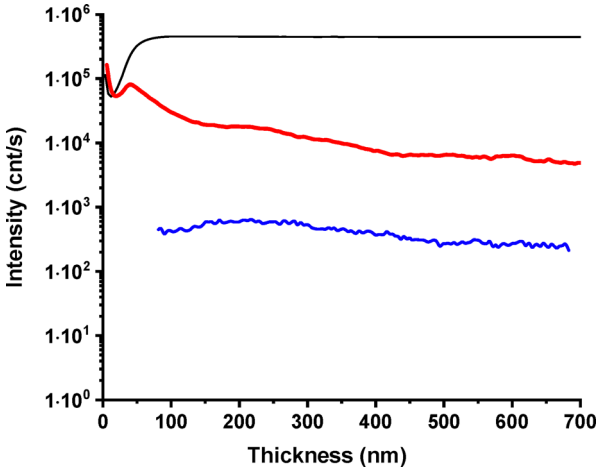

Fig. 13 Elemental composition profile of ^{12}C antibacterial MAB PU (black) and ^{127}I in thin PU without (blue) or with 2 wt% of AB antibacterial copolymers (MAB) (red) obtained by D-SIMS analysis.

for GI-SAXS analyses). The non-mixed material exhibited a scattering profile nearly identical to the reference PU matrix, that could indicate that insufficient incorporation of the copolymer into the network. These results confirm the necessity of pre-compounding to achieve a better copolymer distribution throughout the PU matrix.

For definitive confirmation of copolymer localization, we employed dynamic secondary ion mass spectrometry (D-SIMS), recognized as one of the most sensitive and depth-resolved surface analytical techniques available. Unlike prior studies on PETG and LDPE systems where copolymer detection relied on integrating characteristic fragment peaks (*e.g.*, $m/z \approx 87$ in positive-ion mode) we strategically targeted the ^{127}I isotope as a unique elemental marker. This approach leverages the fact that the antibacterial copolymer undergoes quaternization of its amine groups with methyl iodide, resulting in iodide (I^-) as the counterion to the cationic quaternary ammonium sites. Since iodide is entirely absent from the native PU backbone, its detection constitutes direct and unambiguous proof of copolymer incorporation.

The D-SIMS depth profiles (Fig. 13) reveal significantly higher ^{127}I signal intensity in the 2 wt% copolymer-loaded PU compared to the virgin control, with the iodide concentration remaining nearly constant over a sputtering depth of ~700 nm. This uniformity indicates homogeneous bulk dispersion of the copolymer, while the elevated surface signal relative to deeper regions confirms preferential surface accumulation, a highly desirable feature for contact-active antibacterial materials. For normalization, ^{12}C was used as an internal reference, being abundant in both the PU chains and the copolymer backbone.

These results provide the first conclusive evidence of the antibacterial copolymer's presence both at the surface and throughout the bulk of the co-extruded PU, with enriched surface concentration that directly supports its sustained contact-killing mechanism representing a critical step forward in understanding, optimizing, and validating this scalable antimicrobial platform for medical device applications.

4. Conclusions

Polyurethanes constitute a distinctive class of polymers, distinguished by their multiblock architecture comprising alternating soft and hard segments along the macromolecular chain. This structural hallmark confers exceptional tunability, enabling the tailoring of mechanical properties across a broad continuum from highly elastomeric to rigid and mechanically robust materials while preserving inherent biocompatibility, a key attribute that has cemented their pervasive adoption in medical device fabrication. Nevertheless, despite their critical role in patient care, PU-based devices remain a significant vector for healthcare-associated infections, including nosocomial and device-related infections, underscoring the urgent need for effective antimicrobial strategies.

Conventional approaches to infection prevention have largely relied on leaching systems, wherein active agents such as antibiotics or silver-loaded zeolites are incorporated for controlled release. While widely implemented, these methods suffer from limited durability, potential toxicity, and the risk of promoting antimicrobial resistance. In contrast, surface-grafted antimicrobial functionalities offer sustained activity but demand intricate, costly, and often non-scalable synthetic protocols that pose significant barriers to industrial translation.

In this study, we introduce a simple, robust, and industrially viable strategy based on the dispersion and co-extrusion of just 2 wt% of a quaternary ammonium-based antibacterial copolymer into PU matrices. This approach yields materials with potent, contact-active antibacterial performance without compromising mechanical integrity or biocompatibility. Crucially, we demonstrate full compatibility with essential processing additives such as $BaSO_4$ (for radiopacity) and color

masterbatches (for visual coding), and broad applicability across diverse commercial PU grades, regardless of chemical composition or segmental structure. The resulting materials exhibit remarkable long-term stability, retaining full antibacterial efficacy after three months of aqueous immersion and four successive bacterial challenges (against both Gram-positive and Gram-negative strains), all while remaining non-hemolytic and non-cytotoxic to key mammalian cell types (HaCaT, HUVEC, L929 fibroblast) and erythrocytes.

For the first time, D-SIMS analysis provided direct molecular proof of copolymer incorporation, revealing homogeneous bulk dispersion coupled with preferential surface enrichment, an ideal profile for contact-killing mechanisms. Despite the minimal loading, the additive is unambiguously detectable *via* its ^{127}I counterion, confirming both presence and distribution with nanoscale precision.

Collectively, these findings establish the co-extrusion-based platform as a scalable, additive-compatible, and regulatory-compliant pathway for producing next-generation antibacterial PUs. By overcoming the limitations of traditional methods, this process paves the way for safer, more durable medical devices capable of significantly reducing the burden of nosocomial infections in clinical settings.

Author contributions

Baptiste Caron: investigation, visualization, writing – original draft. Marc Maresca: investigation. Amélie Leroux: conceptualization, resources, supervision. Marie Lemesle: conceptualization, resources, supervision. Jean Louis Coussegal: resources, supervision. Loic Fontaine: investigation, visualization. Elizabeth A. Murphy: investigation. Christopher M. Bates: resources, supervision. Phong H. Nguyen: investigation. Phillip A. Kohl: investigation, supervision. Olivier Soppera: investigation. Stephane Canaan: supervision. Isabelle Poncin: investigation. Yohann Guillaneuf: conceptualization, project administration, writing – review & editing. Catherine Lefay: conceptualization, funding acquisition, project administration, writing – review & editing.

Conflicts of interest

There are no conflicts to declare.

Data availability

The data that support the findings of this study are available from the corresponding author upon reasonable request.

Supplementary information (SI) is available. See DOI: https://doi.org/10.1039/d5tb02613j.

Acknowledgements

The authors thank VYGON, the Centre National de la Recherche Scientifique (CNRS), The SATT Sud-Est and Aix-Marseille Université (AMU) for financial support. VYGON is acknowledged for the PhD funding of Baptiste Caron. C. M. B. thanks the National Science Foundation Award No. CMMI-2053760 for support (characterization experiments). The electron microscopy experiments were performed on the PICsL-FBI core facilty (plateform, IBDM, AMU-Marseille), member of the France-BioImaging national research infrastructure (ANR-24-INBS-0005).

References

1 A. Mishra, A. Aggarwal and F. Khan, *Antibiotics*, 2024, **13**, 16.
2 N. Bouhrour, P. H. Nibbering and F. Bendali, *Pathogens*, 2024, **13**, 52.
3 H. R. Wang, T. Li, J. Li, R. H. Zhao, A. Ding and F. J. Xu, *Prog. Polym. Sci.*, 2024, **151**, 33.
4 K. Navas-Gómez and M. F. Valero, *Materials*, 2020, **13**, 17.
5 C. Casimero, T. Ruddock, C. Hegarty, R. Barber, A. Devine and J. Davis, *Medicines*, 2020, **7**(9), 49.
6 J. Bruenke, I. Roschke, S. Agarwal, T. Riemann and A. Greiner, *Macromol. Biosci.*, 2016, **16**, 647–654.
7 J. A. Grapski and S. L. Cooper, *Biomaterials*, 2001, **22**, 2239–2246.
8 C.-H. Wang, G.-G. Hou, Z.-Z. Du, W. Cong, J.-F. Sun, Y.-Y. Xu and W.-S. Liu, *Polym. J.*, 2015, **48**, 259–265.
9 T. M. Liu, X. Z. Wu and Y. R. Qiu, *J. Biomater. Sci., Polym. Ed.*, 2016, **27**, 1211–1231.
10 Y. Q. Song, Y. L. Gao, X. Y. Wan, F. Luo, J. H. Li, H. Tan and Q. Fu, *RSC Adv.*, 2016, **6**, 17336–17344.
11 E. Udabe, M. Isik, H. Sardon, L. Irusta, M. Salsamendi, Z. Sun, Z. Q. Zheng, F. Yan and D. Mecerreyes, *J. Appl. Polym. Sci.*, 2017, **134**, 7.
12 Y. D. Zhang, X. Zhang, Y. Q. Zhao, X. Y. Zhang, X. K. Ding, X. J. Ding, B. R. Yu, S. Duan and F. J. Xu, *Biomater. Sci.*, 2020, **8**, 997–1006.
13 Y. L. Yuan, F. Ai, X. P. Zang, W. Zhuang, J. Shen and S. C. Lin, *Colloid Surf., B*, 2004, **35**, 1–5.
14 M. Khan, Y. K. Feng, D. Z. Yang, W. Zhou, H. Tian, Y. Han, L. Zhang, W. J. Yuan, J. Zhang, J. T. Guo and W. C. Zhang, *J. Polym. Sci. Polm. Chem.*, 2013, **51**, 3166–3176.
15 Y. F. Qian, J. Zhao, L. Liu, H. Hu, B. Wang and H. Y. Zhang, *Langmuir*, 2022, **38**, 3597–3606.
16 Y. L. Zhao, Y. F. Qian, H. M. Wang, W. W. Zhao, J. Zhao and H. Y. Zhang, *ACS Appl. Polym. Mater.*, 2023, **5**, 3999–4010.
17 J. S. Zhang, S. Y. Lv, X. D. Zhao, S. H. Ma and F. Zhou, *Adv. Colloid Interface Sci.*, 2024, **325**, 103100.
18 B. T. Benkhaled, S. Hadiouch, H. Olleik, J. Perrier, C. Ysacco, Y. Guillaneuf, D. Gigmes, M. Maresca and C. Lefay, *Polym. Chem.*, 2018, **9**, 3127–3141.
19 B. Caron, M. Maresca, A. Leroux, M. Lemesle, J. L. Coussegal, Y. Guillaneuf and C. Lefay, *Macromol. Rapid Commun.*, 2024, **45**, 9.
20 S. Hadiouch, M. Maresca, D. Gigmes, G. Machado, A. Maurel-Pantel, S. Frik, J. Saunier, A. Deniset-Besseau, N. Yagoubi, L. Michalek, C. Barner-Kowollik, Y. Guillaneuf and C. Lefay, *Polym. Chem.*, 2022, **13**, 69–79.
21 S. H. Hsu, H. J. Tseng and Y. C. Lin, *Biomaterials*, 2010, **31**, 6796–6808.

